

The formation of vortex loops (strings) in continuous phase transitions

Mark J. Bowick^{(1)*}, Angelo Cacciuto^{(1)†} and Alex Travesset^{(2)‡}

¹ Physics Department, Syracuse University,
Syracuse NY 13244-1130, USA

² Loomis Laboratory, University of Illinois at Urbana,
Urbana IL 61801, USA

Abstract

The *formation* of vortex loops (global cosmic strings) in an $O(2)$ linear sigma model in three spatial dimensions is analyzed numerically. For over-damped Langevin dynamics we find that defect production is suppressed by an interaction between correlated domains that reduces the effective spatial variation of the phase of the order field. The degree of suppression is sensitive to the quench rate. A detailed description of the numerical methods used to analyze the model is also reported.

*bowick@physics.syr.edu

†cacciuto@physics.syr.edu

‡travesse@uiuc.edu

Introduction

The mechanism by which topological defects form in continuous phase transitions has been a fascinating field of research for many years with implications for astroparticle cosmology, particle physics and condensed matter systems [1–5]. On the cosmological side it is very likely that the universe underwent a sequence of symmetry-breaking phase transitions during its expansion and subsequent cooling after the Big-Bang. If the disordered phase has symmetry G and the ordered phase a lower symmetry H then the manifold \mathcal{M} of possible vacua is given by the coset space G/H . In many cases the vacuum manifold \mathcal{M} has some non-trivial topology, allowing for the appearance of topological defects corresponding to the non-vanishing homotopy classes of \mathcal{M} . In realistic (finite quench rate) continuous phase transitions, critical slowing down then implies that there must be some time during the transition at which the intrinsic ordering dynamics becomes too sluggish to keep pace with the quench. It is then inevitable that some neighboring domains will form with an orientation that produces topological defects as they coalesce.

On the condensed matter side, where phase transitions occur in accessible and reproducible laboratory conditions, the production of topological defects is familiar and observed in, for example, ferromagnets [6], liquid crystals [7–11] and superfluids (both 4He [12–14] and 3He [15, 16]).¹ Most of the work on defects in condensed matter systems has focused on either the classification of defects [6, 17–19], or the coarsening dynamics governing the late-time evolution of the defect density [3]. But it is also of considerable interest to determine the precise mechanism by which defects are produced and to determine the defect density *at* formation [5, 20, 21]. This is the problem tackled in this paper for the case of the linear $O(2)$ sigma model, for which \mathcal{M} is the circle S^1 . We examine numerically the process of defect production in fixed-rate quenches through the formation, interaction and coalescence of interacting domains with well-defined phases and determine the defect density *at* the time of production.

We find there is considerable phase alignment of domains between their formation and the subsequent production of defects. The spatial variation of the phase is then smoother than one would obtain from assuming that domains are statistically independent. In other words the wandering of the

¹The most recent improved experiments of the Lancaster group on the fast adiabatic expansion of liquid 4He through the superfluid λ transition [14] do not see any vortex lines, in contrast to their earlier results [12].

phase on the ground state manifold S^1 from domain to domain is not random – domains of a given phase attract other domains with similar phases. This clearly reduces the likelihood that domain coalescence will yield a topological defect.

Although classical and quantum-mechanical continuous phase transitions have been modelled and systematically investigated, both analytically [5, 20–27] and numerically [28–33], a complete understanding is still lacking.

The remainder of the paper consists of five sections. In section 1 we review mechanisms for the production of topological defects in continuous phase transitions. In section 2 we define the problem at hand and outline our approach. Section 3 gives the details of the numerical analysis performed and section 4 gives our results. Finally we conclude and discuss some possible implications of our work.

1 The Kibble-Zurek mechanism

In the Ginzburg-Landau picture continuous phase transitions proceed through the growth of arbitrarily small amplitude, long-wavelength fluctuations — the so-called spinodal decomposition of the *unstable* symmetric phase to the true ordered phase. These spinodal modes grow exponentially in time until cutoff by the nonlinearities associated with interactions. When a system undergoing a continuous phase transition is quenched at a finite rate from the disordered to the ordered phase, distinct ordered regions of space (**domains**) will generically lie at different points on the vacuum manifold.

In [20] Kibble proposed a clear mechanism for topological defect formation in a cosmological context using a simple ordering-causality argument. The key idea is that spontaneous symmetry breaking will occur independently in causally disconnected regions of space. Suppose that order parameter is uniform within an ordered domain of correlation volume ξ^3 and randomly distributed on the ground-state (vacuum) manifold \mathcal{M} . Furthermore Kibble assumed that the order parameter between domains was the smoothest interpolation possible (the *geodesic rule*). In this case one can, in principle, compute the probability that the coalescence of say three domains leads to a topologically non-trivial configuration. This probability is a number of order one so that, roughly speaking, one defect is formed per correlation volume.

To predict the density of defects at formation in this picture one must have a theory of the relevant correlation length ξ at formation. One simple

proposal [20] is that ξ corresponds to the correlation length at the Ginzburg temperature (T_G) when ordered domains are stable to thermal fluctuations. Given the free energy barrier ΔF (see Fig. 1) between the true ground state and the unstable high-temperature phase for $T < T_c$, we have

$$k_B T_G \simeq \xi^3(T_G) \Delta F(T_G). \quad (1)$$

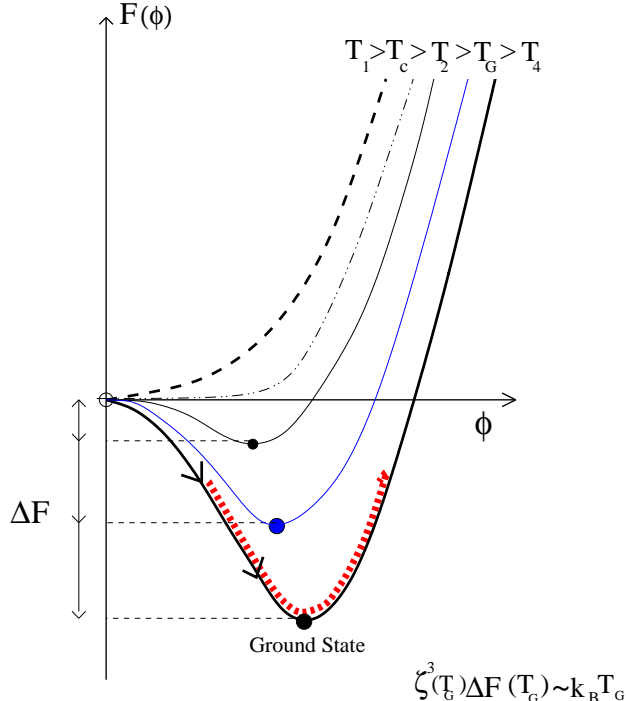


Figure 1: Schematic representation of the free energy curve showing the disordered ($T > T_c$) and ordered ($T < T_c$) phases for a scalar field ϕ in a $\lambda\phi^4$ theory. The highlighted dashed section indicates typical thermal fluctuations for temperatures below the Ginzburg temperature $T < T_G$.

Above T_G the system can locally jump back and forth between the high and low temperature phases. Below T_G this process is thermally suppressed.

This argument ignores the dynamical aspects of the phase transition and is likely to be inaccurate if defects form at relatively high temperatures. An alternative *non-equilibrium* approach was proposed by Kibble in a later paper [21] and elaborated by Zurek [5]. Consider a continuous phase transition proceeding with a finite quench rate. The quench may be an externally imposed

temperature or pressure quench or result from the expansion of the universe in the cosmological setting. In the ordered phase a given region of space may attain the ground state as long as the microscopic dynamics enables it to relax more rapidly than the quench rate. But in a continuous transition critical slowing down implies that the intrinsic relaxation rate becomes arbitrarily slow near the critical temperature. Thus there is a characteristic time or temperature at which the system cannot order sufficiently rapidly. The correlation length at this time provides an estimate of the maximum domain size giving rise to topological defects. In causal language typical domain sizes cannot grow faster than the speed of light and therefore can never attain the infinite correlation lengths associated with the critical point.

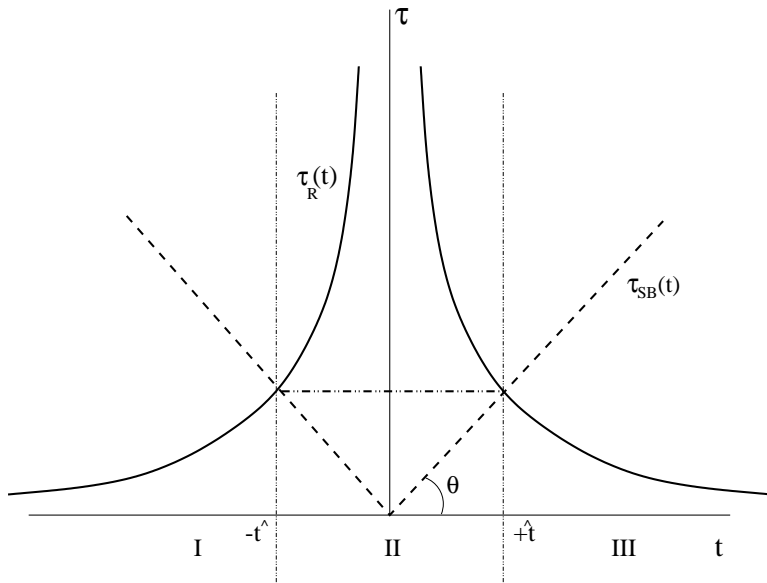


Figure 2: Schematic representation of the relaxation time $\tau_R(t)$ versus the symmetry breaking time $\tau_{SB}(t)$ of a system being quenched through a continuous phase transition at a rate $1/\tau_Q$.

This picture is illustrated in Fig. 2. The two time scales in the problem are the relaxation time $\tau_R(t)$ and the symmetry breaking time $\tau_{SB}(t)$ (here taken to be linear). The dynamics may be divided in three stages. For $t \ll -\hat{t}$ (stage I) the relaxation time of the system is smaller than $\tau_{SB}(t)$. The field can dynamically relax to equilibrium while the temperature is falling. When $t \sim -\hat{t}$, the symmetry breaking time and the relaxation time become

comparable and when $-\hat{t} < t < \hat{t}$, the situation is reversed. During stage II $\tau_{SB}(t) \ll \tau_R(t)$, and the time needed by the system to relax to equilibrium is much larger than the symmetry breaking time. The system cannot relax and the correlation length ξ cannot grow as the critical point is approached. Its value is frozen until, for $t > \hat{t}$, $\tau_{SB}(t) > \tau_R(t)$ (stage III) where ξ eventually decreases as expected in the ordered phase. The faster the quench rate τ_Q , the smaller the angle θ indicating the slope of $\tau_{SB}(t)$. Consequently, the maximum value reached by ξ will be smaller and smaller, creating a higher defect density. The slower the quench rate, the larger θ . ξ is allowed to grow to larger values while approaching the critical point and the density of defects that form will be smaller (spatially correlated regions have on average a larger size). Assuming that the correlation length at formation is the one relative to $t = \hat{t}$, (we can safely assume that $\xi(-\hat{t}) \simeq \xi(\hat{t})$), it is easy to show that a power law dependence between the freeze-out correlation length ξ^* and the quench rate τ_Q of the phase transition holds

$$\xi^* \sim (\tau_Q)^{\frac{\nu}{\mu+1}}, \quad (2)$$

where $\tau_R(t) \sim |\varepsilon|^{-\mu}$, $\xi \sim |\varepsilon|^{-\nu}$ and $\varepsilon = t/\tau_Q$. Extensive analytical and numerical checks have lent support to the Kibble-Zurek mechanism (see references in the introduction).

2 Interacting Ordered Domains

In this paper we will model the ordering kinetics of a non-conserved order parameter by Langevin dynamics with a global $O(2)$ ϕ^4 Ginzburg-Landau free energy functional. We will not treat gauge theories [34]. The order parameter $\bar{\phi}$ is zero in the high-temperature disordered phase and non-zero in the low-temperature ordered phase. For a continuous transition $\bar{\phi}$ switches on continuously. We model the thermal quench via a linearly time varying mass term with slope τ_Q .

$$F(|\phi|) = \int d^d r \left[\frac{1}{2}(|\nabla \phi|)^2 + V(|\phi|) \right], \quad (3)$$

with a potential of the form

$$V(|\phi|) = \frac{1}{2}m^2(t)|\phi|^2 + \frac{1}{4}\lambda|\phi|^4 \quad (\lambda > 0) \quad (4)$$

For $m^2(t) \geq 0$, $|\phi| = 0$ and for $m^2(t) < 0$, $|\phi| = \pm m(t)/\lambda^{1/2}$. In the broken-symmetry phase

$$\phi = \rho e^{i\theta} \quad (5)$$

where $\rho \equiv |\phi|$ and θ is a phase chosen from the ground-state manifold S^1 .

Below the critical point ordering progresses via the formation of ordered domains within which the phase is constant. Topological defects form as domains coalesce, as described in the Introduction.

When identifiable stable domains first form they are widely separated. Between the time they form and the time they coalesce to produce defects one may expect considerable interaction to take place since we are dealing with a non-linear field theory. Indeed angular gradient terms in the broken symmetry regime of the free-energy should align phases from one domain to the next. This will suppress wandering of the phase on the ground-state manifold and lower the probability of forming defects. This is the effect we establish and quantify in this paper.

3 Counting Defects: A numerical approach.

In this section we discuss how we count topological defects numerically. We first define an oriented (ordered) domain on the lattice as the ensemble of spatially connected sites whose phase difference satisfies the constraint $|\Delta\theta| < \theta_\varepsilon$, where we have introduced a cutoff angle θ_ε . The number of domains at a given time is strongly dependent on the value of θ_ε . Choosing θ_ε too small will result in too many domains that are unstable to thermal fluctuations. Taking θ_ε too large, on the other hand, means we can no longer properly track the spatial variation of the phase. The best compromise is achieved by choosing the largest possible value of θ_ε that preserves the topology of the system. In other words, we look for the effective domains whose coalescence closely matches the distribution of defects obtained from the *full* field. To be specific we take a Z_n discretization of the circle into n slices $\alpha(k)$ ($k = 0, 1, \dots, n-1$) of width $\Delta = 2\pi/n$ and coarse grain the angular part of the field as follows

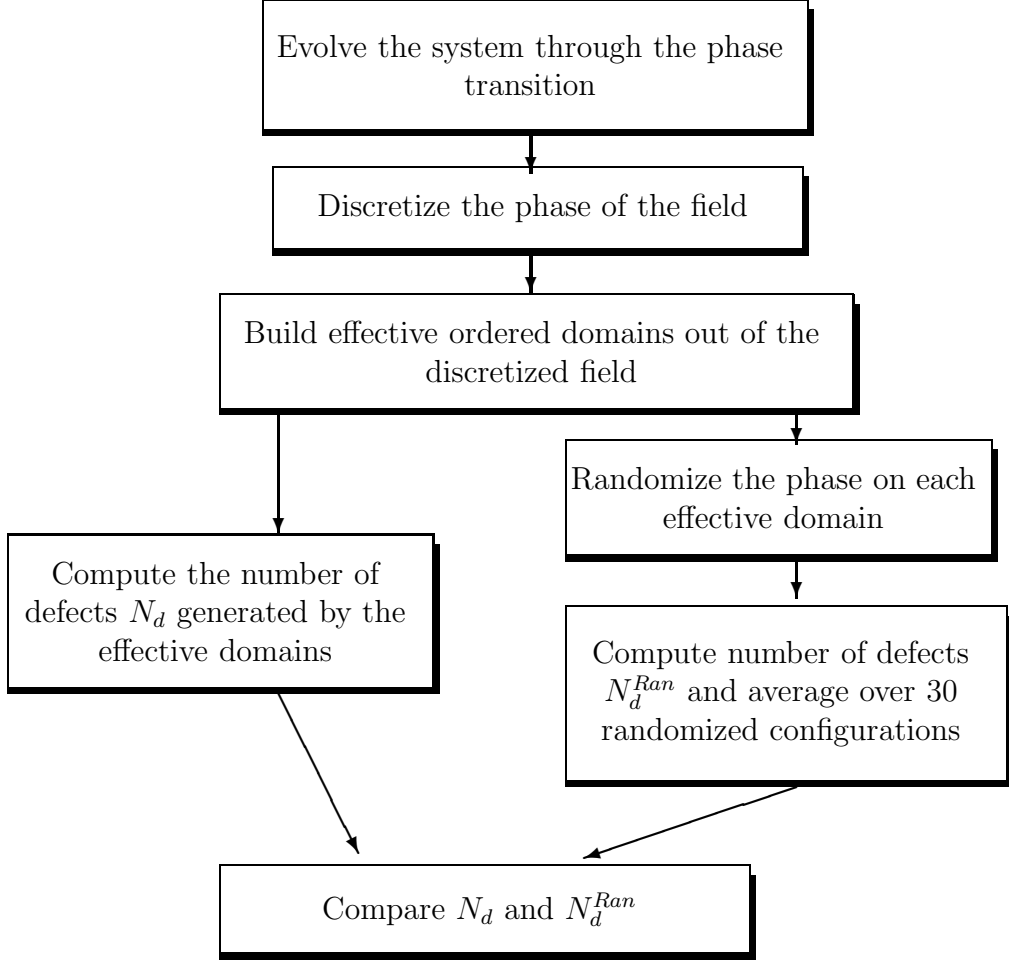
$$\theta_i = \Theta^{\alpha(k)} \quad \text{if } \theta_i \in \alpha(k) \quad (6)$$

where i is the lattice site and

$$\Theta^{\alpha(k)} = \frac{1}{2} (k\Delta + (k+1)\Delta) \quad k = 0, 1, \dots, n-1. \quad (7)$$

We then compute the number of defects using this coarse grained field configuration and compare it to that obtained using continuous angles. We find that the largest Δ that preserves the topology is $\pi/4$, corresponding to a Z_8 discretization. The error in the defect count resulting from this discretization is on average smaller than 5%.

We also address the stability of domains to thermal fluctuations. For this purpose we introduce a minimum domain size (cut-off) Λ_b . The system is kept in contact with a heat bath at constant temperature T ($T \ll T_c$) throughout the simulation. Λ_b is chosen to be the largest spatially connected domain generated by thermal fluctuations in the disordered phase. We now have all necessary tools to explore the dynamics of the effective domains. The following schematic illustrates our strategy:



The third stage requires more details. Since we introduced a minimum domain size Λ_b , very few domains will form in the early stages of ordering. Only a small fraction of the lattice is ordered. One may ask whether these domains have the expected random distribution of phases. To test this we simultaneously grow each domain by adding an outer shell of sites of width equal to one lattice site with the same field phase. We then recursively grow each domain's external surface until they meet in the same region of space and the complete lattice is filled (see Fig. 3 for an illustration of this algorithm applied to a two-dimensional configuration). The final configuration obtained by this construction corresponds to freely expanding domains with

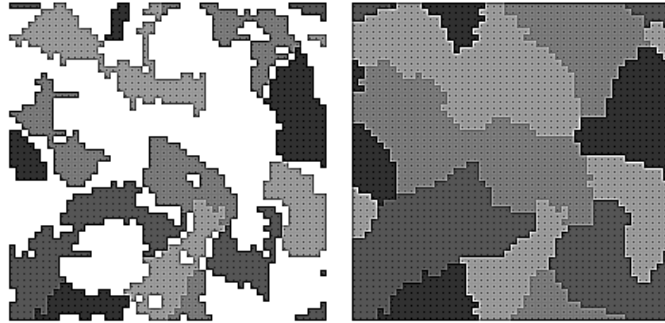


Figure 3: Two dimensional example of the domain reconstruction procedure. The left image represents a discretized configuration on a 50×50 lattice (periodic boundary conditions) with a given bubble cut-off Λ_b , and the right image is its layer by layer reconstructed configuration. Each color represents a different phase of the field.

fixed phases. If phases are randomly distributed across domains the number of defects determined before and after randomizing should be statistically equivalent. As the quench progresses more domains are created over the lattice. We repeat the same procedure at each time step of the evolution until almost all the lattice is filled with well-defined domains. A domain-domain interaction will be traceable by comparing the number of defects produced. In particular the difference between the actual number of defects and the number for the random distribution of phases should grow with time, reaching a maximum at the time of domain coalescence.

To resolve strings on the lattice we follow [28] and associate a vortex to each lattice plaquette with a non-trivial phase winding. Strings are then constructed by connecting these vortices, adopting a random reconnection algorithm for the case of multiple strings passing through the same lattice cell. To deal with this ambiguity the number of strings at each time step is obtained by averaging over 15 differently recombined string configurations ². All simulations were performed on a 300MHz Pentium II for a total computational time of roughly 800 hours.

²The uncertainty in this counting is smaller when the phases are discretized.

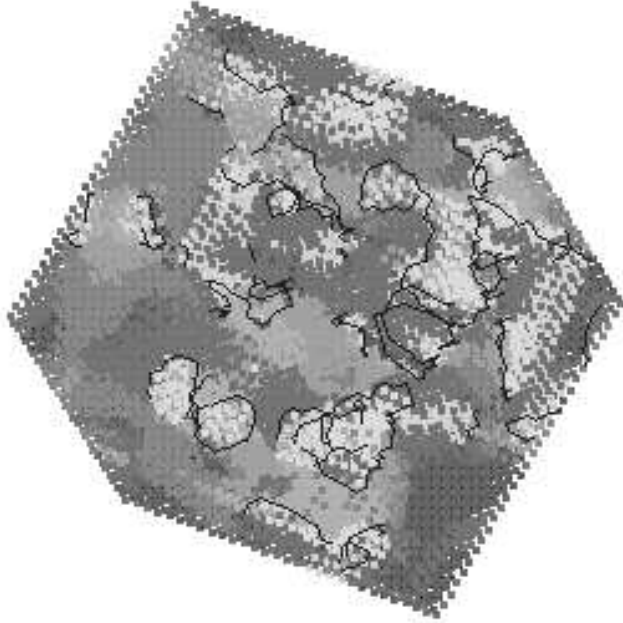


Figure 4: A snap-shot of a typical configuration of the system in a 3D, $L = 30$, lattice with periodic boundary conditions. Each color represents a different phase of the field. Dark lines represent the string defects trapped between the ordered domains.

4 Numerical simulation

We simulated a two-component classical vector field $\vec{\phi}(\vec{r})$ on a three dimensional cubic lattice of side $L = 60$ with periodic boundary conditions. We evolve the system using a leap-frog numerical implementation of the Langevin equation in the over-damped regime

$$\frac{1}{\Gamma_0} \frac{\partial \vec{\phi}}{\partial t} = \vec{\nabla}^2 \vec{\phi} - \frac{\partial V(\vec{\phi})}{\partial \vec{\phi}} + \vec{\eta}(\vec{r}, t) \quad (8)$$

where Γ_0 is a dimensionful constant, $V(\vec{\phi})$ is given in Eq.(4) and $\vec{\eta}(\vec{r}, t)$ is Gaussian noise with temperature T that satisfies the following constraints

$$\langle \eta_a(\vec{r}, t) \rangle = 0 \quad (9)$$

and

$$\langle \eta_a(\vec{r}_1, t_1) \eta_b(\vec{r}_2, t_2) \rangle = 2T\Gamma_0 \delta_{ab} \delta(\vec{r}_1 - \vec{r}_2) \delta(t_1 - t_2). \quad (10)$$

It is convenient to rescale to dimensionless variables, to be used from now on, as follows

$$\begin{aligned} x' &= m_0 x & t' &= m_0 t & \eta' &= \eta \sqrt{\lambda} / (m_0^3) \\ T' &= T \lambda / m_0 & \phi' &= \phi \sqrt{\lambda} / m_0. \end{aligned} \quad (11)$$

where m_0 is the value of $m(t)$ prior the quench; when the system is in the symmetric phase. The rescaled equation, dropping the primes, then becomes

$$\partial_t \phi = \nabla^2 \phi - \alpha(t) \phi - \phi^3 + \eta \quad (12)$$

where $\alpha(t) = m^2(t)/m_0^2$ and we have chosen $\Gamma_0 m_0 = 1$. The linear quench is modeled by

$$\alpha(t) = \begin{cases} 1 & \text{for } t \leq 0 \\ (1 - 2\frac{t}{\tau_Q}) & \text{for } 0 \leq t \leq \tau_Q \\ -1 & \text{for } t \geq \tau_Q \end{cases} \quad (13)$$

τ_Q^{-1} being the quench rate. This choice of $\alpha(t)$ enables us to drive the system from a disordered phase (convex potential) to an ordered phase (sombrero-like potential) in a finite time. For $t < 0$ the system is in thermal equilibrium in the disordered phase. As $0 \leq t \leq \tau_Q$, $\alpha(t)$ linearly decreases until it changes sign passing through the critical point. When $t \geq \tau_Q$, $\alpha(t)$ stops decreasing terminating the quench into the ordered phase. The limit $\tau_Q \rightarrow 0$ corresponds to an instantaneous quench while $\tau_Q \rightarrow \infty$ describes an adiabatic quench. Throughout the simulation the rescaled heat bath temperature T is held constant. We scanned temperatures ranging from $T = 0.001$ to $T = 0.1$. The results reported here are for $T = 0.035$. The equations were numerically solved using $\Delta x = 0.5$ and $\Delta t = 0.1$.

In the subsequent analysis we first treat instantaneous quenches and then compare to the results for a slow quench.

4.1 Instantaneous Quench: $\tau_Q = 0$

We let the system equilibrate in the disordered phase ($\alpha(t) = 1$, $\langle \phi \rangle = 0$) in the presence of thermal noise η at $T = 0.035$. We sample over 1000 thermalized configurations to get the minimum ordered domain cut-off Λ_b , as previously described. At this temperature and this lattice size ($L=60$) we

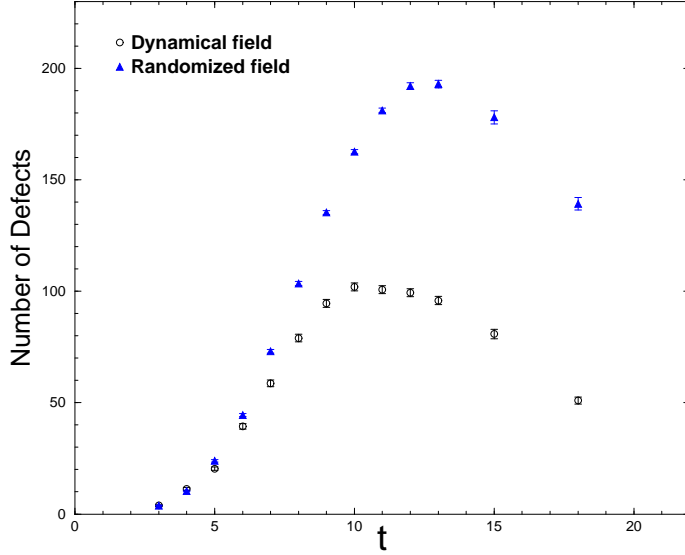


Figure 5: Number of defects generated by the discretized field compared to the random-discretized field in an instantaneous quench ($\tau_Q = 0$).

find that the largest thermally generated bubble in the high temperature phase has a volume of $V_b \equiv \Lambda_b = 79$ spatially connected sites. We then switch $\alpha(t) = 1 \rightarrow \alpha = -1$. This breaks the $O(2)$ symmetry and the system evolves toward its equilibrium value $\langle \phi \rangle = 1$ following the equations of motion defined in Eq.12. We calculate the number of defects as explained in section 3. For each simulation we average the number of defects over 50 different randomized configurations at each time step in the dynamics. The number of defects so obtained is then averaged over a sample of 30 different configurations obtained from simulations with different random initial conditions.

Fig. 5 illustrates the results of the analysis. At early times the number of defects produced by both randomized and non-randomized configurations agrees within statistical accuracy. This establishes that the order parameter is randomly varying from one spatial domain to another. At later times the randomized field configurations produce more and more defects with respect

to its counterpart. This clearly indicates that phase alignment is occurring as the domains grow. The gap between the two curves widens until it reaches a maximum at $t = t^* = 12 \pm 1$. We associate this particular time with the time of defect formation. This is supported by the fact that the number of strings generated by the effective domains reaches its maximum value at this same time. The number of strings subsequently decreases as domains coalesce and defects decay. The actual suppression factor in the number of strings formed is given by $\gamma = 2.0 \pm 0.2$. We would like to emphasize that this value should be considered as a lower bound. While counting the number of strings we scanned our data using different minimum string length cut-offs $\Lambda_s = 4, 6, 8, 10, 12, 15, 18, 22$. The data reported above reflect the analysis obtained with $\Lambda_s = 15$. Smaller values of Λ_s slightly increase the value of γ , but also risk over-count defects because many of the smaller strings could be very short-lived. Larger values of Λ_s do not produce a detectable change in γ .

4.2 Slow Quench: $\tau_Q = 50$

We now consider the effects of a finite-rate quench. We first equilibrate in the disordered phase ($\alpha(t) = 1$, $\langle \phi \rangle = 0$) in the presence of thermal noise η at $T = 0.035$ and then initiate the linear quench according to Eq. 13. The longer time interval over which domains interact, that between the time they form and the time of defect production, results in a greater mismatch between the number of defects formed and the idealized random scenario. Of course this difference will disappear in the extreme adiabatic limit as no defects are produced at all in this equilibrium setting. We expect therefore that there is some finite quench rate which maximizes the suppression of defect density. We explored $\tau_Q = 50$ as a quench rate fast enough to produce a large number of defects but still far from the adiabatic limit. The results are given in Fig. 6. As previously discussed, the gap between the two curves grows with time until it reaches a maximum value after which it falls off. It is revealing to compare Fig. 5 and Fig. 6 to understand the main physical difference between the two experiments. It is obvious that the maximum gap between the two curves has widened with respect to the instantaneous quench. We estimate the formation time to be $t^* = t = 30 \pm 2$ and $\gamma = 4.1 \pm 0.4$. The suppression factor γ basically doubles while passing from $\tau_Q = 0$ to $\tau_Q = 50$. There is clearly a relationship between γ and τ_Q . As previously discussed we expect that for $\tau_Q \rightarrow \infty$, $\gamma(\tau_Q) \rightarrow 0$ and would be very interesting to

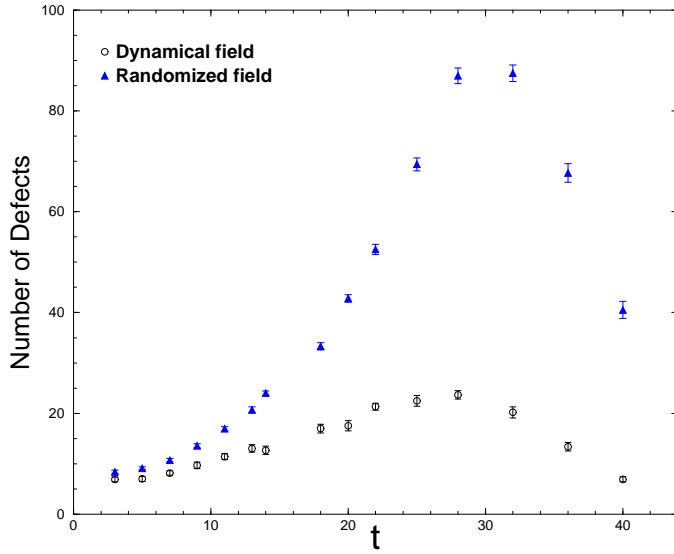


Figure 6: Number of defects generated by the discretized field compared to the random-discretized field in a slow quench ($\tau_Q = 50$).

extrapolate the value of τ_Q that maximizes $\gamma(\tau_Q)$ but the extremely long computational time required to achieve this result is prohibitive.

5 Conclusion and Discussion

In this paper we have analyzed the effect of a finite quench rate on the density of topological defects at formation. Detailed numerical simulations show that the phase angle of ordered domains aligns in the interval between domain formation and the production of defects. The effect of this alignment is to reduce the number of defects that form compared to the simple Kibble mechanism which assumes that domains are statistically independent at the time of coalescence. A lower bound on this relative suppression factor is estimated to be $\gamma = 2.0 \pm 0.2$ for an instantaneous quench and $\gamma = 4.0 \pm 0.4$ for a phase transition with quench time $\tau_Q = 50$. It would be of great interest to systematically vary τ_Q to determine the quench rate with optimal

defect suppression. As τ_Q increases one has to explore larger correlation lengths which is computationally more demanding. We hope to undertake this challenge in the near future.

Our results uncover a new underlying feature of defect formation mechanism that may turn out to play an important role in the precise determination of the initial density of defects generated in a continuous phase transition, a subject of great interest from both the cosmological and condensed matter viewpoint. Our study is most directly applicable to over-damped condensed matter systems but we think that an analogous effect exists in the under-damped regime more appropriate to a relativistic theory. An analysis in this direction is underway.

6 Acknowledgements

The work of MJB, AC and AT was supported by the US Department of Energy (DOE) under contract No. DE-FG02-85ER40237. The work of AT was also supported by funding from the materials computation center, grant NSF-DMR 99-76550 and NSF grant MDMR-0072783.

References

- [1] R. J. Rivers in, *Formation and Interactions of Topological Defects* (Proc. of the NATO Advanced Study Institute on *Topological Defects*, Newton Institute, Cambridge 1994), eds. A-C. Davis and R. H. Brandenberger, p. 139 (Plenum Press, 1995).
- [2] T. Vachaspati, *Lectures on Cosmic Topological Defects*, (Lectures at the 2000 summer school in cosmology at ICTP, Trieste), (e-print: hep-ph/0101270).
- [3] A. Bray, *Adv. Phys.* **43** (1994) 357 (e-print: cond-mat/9501089).
- [4] R. H. Brandenberger and A-C. Davis, *Phys. Lett.* **B332** (1994) 305 (e-print: hep-ph/9403269).
- [5] W. H. Zurek, *Nature* **317** (1985) 505, *Acta Physica Polonica* **B24** (1993) 1301, *Phys. Rep.* **276** (1996) 177 (e-print: cond-mat/9607135).

- [6] D. Mermin, *Rev. Mod. Phys.* **51** (1979) 591.
- [7] S. Chandrasekhar and G.S. Ranganath, *Adv. Phys.* **35** (1986) 507.
- [8] P.G. de Gennes and J. Prost, *The Physics of Liquid Crystals*: Second Edition (Clarendon, Oxford, 1993).
- [9] M. Bowick, L. Chandar, E. Schiff and A. Srivastava, *Science* **263** (1994) 943 (e-print: hep-th/9208233).
- [10] I. Chuang, R. Durrer, N. Turok and B. Yurke, *Science* **251** (1991) 1336.
- [11] I. Chuang, N. Turok and B. Yurke, *Phys. Rev. Lett.* **66** (1991) 2472.
- [12] P. C. Hendry, N. S. Lawson, P. V. E. McClintock and C. D. H. Williams, *Nature* **368** (1994) 315.
- [13] M. E. Dodd, P. C. Hendry, N. S. Lawson, P. V. E. McClintock and C. D. H. Williams, *Expansion of liquid ^4He through the Lambda Transition*, *J. Low Temp. Physics* **115** (1999) 98 (e-print: cond-mat/9810107).
- [14] M. E. Dodd, P. C. Hendry, N. S. Lawson, P. W. E. McClintock and C. D. H. Williams, *Nonappearance of Vortices in Fast Mechanical Expansion of Liquid ^4He through the Lambda Transition*, *Phys. Rev. Lett.* **81** 3703(1998) (e-print: cond-mat/9808117).
- [15] V. M. Ruutu, V. B. E. Eltsov, A. T. Gill, T. W. B. Kibble, M. Krusius, Yu. G. Makhlin, B. Plaçais, G. E. Volovik, Wen Xu, *Nature* **382** 334 (1996) (e-print: cond-mat/9512117).
- [16] V. M. Ruutu, V. B. Eltsov, M. Krusius, Yu. G. Makhlin, B. Plaçais and G. E. Volovik, *Defect Formation in Quenched-Cooled Superfluid Phase Transition*, *Phys. Rev. Lett.* **80** (1998) 1465 (e-print: cond-mat/9706038).
- [17] M. Kleman, *Points, Lines and Walls in Liquid Crystals, Magnetic Systems and Various Ordered Media* (Wiley, Chichester, 1983).
- [18] L. Michel, *Symmetry defects and broken symmetry*, *Rev. Mod. Phys.* **52** (1980) 617.

- [19] Y. Bouligand, in *Les Houches Session XXXV, Physics of Defects*, R. Balian, Ed. (North-Holland, Dordrecht, Netherlands, 1981).
- [20] T. W. B. Kibble, *J. Phys.* **A9** (1976) 1387.
- [21] T. W. B. Kibble, *Phys. Rep.* **67** (1980) 183.
- [22] A. J. Bray, *Defect Relaxation and Coarsening Exponents*, *Phys. Rev.* **E58** (1998) 1508 (e-print: cond-mat/9802183).
- [23] R. J. Rivers, *Fluctuations and Phase Transition Dynamics*, *Int. J. Theor. Phys.* **39** (2000) 1779 (e-print: hep-ph/0001197).
- [24] D. Boyanovsky, D.S. Lee and A. Singh, *Phys. Rev.* **D 48** (1993) 800 (e-print: hep-ph/9212083); D. Boyanovsky, *Phys. Rev.* **E 48** (1994) 767 (e-print: hep-ph/9301095).
- [25] M. Bowick and A. Momen, *Domain formation in finite-time quenches*, *Phys. Rev.* **D 58** (1998) 085014 (e-print: hep-ph/9803284).
- [26] G. Karra and R. J. Rivers, *Phys. Lett.* **B 414** (1997) 28 (e-print: hep-ph/9705243).
- [27] D. Boyanovsky, H. G. De Vega and R. Holman, *Non-Equilibrium Phase Transitions in Condensed Matter and Cosmology: Spinodal Decomposition, Condensates and Defects*; lectures delivered at the NATO Advanced Study Institute: *Topological Defects and the Non-Equilibrium Dynamics of Symmetry Breaking Phase Transitions*, (e-print: hep-ph/9903534).
- [28] T. Vachaspati and A. Vilenkin, *Phys. Rev.* **D 30** (1984) 2036.
- [29] M. Gleiser and H.R. Müller, *Phys. Lett.* **B 422** (1998) 69 (e-print: hep-lat/9704005).
- [30] D. Ibáñez and E. Calzetta, *Phys. Rev.* **E 60** (1999) 2999 (e-print: hep-ph/9810301).
- [31] N. D. Antunes and L. M. A. Bettencourt, *Phys. Rev.* **D 55** (1997) 925 (e-print: hep-ph/9605277).

- [32] N. D. Antunes, L. M. A. Bettencourt and W. H. Zurek, *Phys. Rev. Lett.* **82** (1999) 2824 (e-print: hep-ph/9811426).
- [33] C. J. Gagne and M. Gleiser, *Quantifying Nonequilibrium Behavior with Varying Cooling Rates* (e-print: cond-mat/0105503).
- [34] For a recent review of defect formation in gauge theories, see A. Rajantie, e-print:hep-ph/0108159.